

# Programming Multistate Aggregation-Induced Emissive Polymeric Hydrogel into 3D Structures for On-Demand Information Decryption and Transmission

Huiyu Qiu, Shuxin Wei, Hao Liu, Beibei Zhan, Huizhen Yan, Wei Lu,\* Jiawei Zhang, Si Wu, and Tao Chen\*

Fluorescent hydrogels have recently become one of the most prominent materials for smart confidential information protection. But it is still quite challenging to develop a 3D anticounterfeiting platform with on-demand information decryption and transmission capacities, which are of great importance to achieve high-level data protection security. Herein, robust aggregation-induced emissive polymeric hydrogels with thermo-triggered multistate fluorescence switching, shape memory, and self-healing properties based on supramolecular dynamic lanthanide coordination interactions are presented. By a collective action of these promising properties, a fluorescent hydrogel-based 3D information encoding platform is demonstrated for on-demand information decryption, in which information pre-encrypted in 3D hydrogel structures is stepwise decrypted by the control of external stimuli. Such unique on-demand information decryption features are further expanded to the transmission of manifold customized messages to multiple receivers. Herein, the possibility of utilizing 3D fluorescent hydrogel structures for high-level information encryption and on-demand decryption is opened up.

wide color tunability.<sup>[2]</sup> To date, a number of chromophoric and luminescent materials have been developed as security inks or solid-state data carriers (e.g., polymeric films) to protect confidential documents, banknotes, as well as high-value merchandise. Nevertheless, compared with the classic materials with static color or emission outputs, advanced materials with dynamic color or emission possibilities would offer better performances and extra levels of security or quantity of coded data. Therefore, there has been a recent research trend toward such stimuli-responsive materials with multistate switching of optical properties to significantly improve the security level of the encoded texts, because they are favorable to achieve the desirable on-demand decryption behavior, in which different information would appear at different conditions.<sup>[3]</sup> For example, Huang, Zhao, and coworkers presented a series

## 1. Introduction


Information security protection and transmission play important roles in military, commercial, and even daily-life activities.<sup>[1]</sup> One promising chemistry-related anticounterfeiting technique is to encrypt information by chromophoric or luminescent materials due to their multiple advantages such as facile availability and

of spirolactam-containing zinc complexes with varying photochromic rates by changing counterions and demonstrated their use as photochromic films for multilevel security printing on 2D paper substrates, in which different information could be decoded at various irradiation times.<sup>[3a]</sup> Zhao, Yan, and colleagues reported a strategy to realize multiple lasing states for high-level optical encryption by regulating the competition

H. Qiu, S. Wei, H. Liu, B. Zhan, H. Yan, Prof. W. Lu, Prof. J. Zhang, Prof. T. Chen  
 Key Laboratory of Marine Materials and Related Technologies  
 Zhejiang Key Laboratory of Marine Materials and Protective Technologies  
 Ningbo Institute of Materials Technology and Engineering  
 Chinese Academy of Sciences  
 Ningbo 315201, China  
 E-mail: luwei@nimte.ac.cn; tao.chen@nimte.ac.cn

H. Qiu  
 Nano Science and Technology Institute  
 University of Science and Technology of China  
 No. 166 Renai Road, Suzhou 215000, China

S. Wei, H. Liu, Prof. W. Lu, Prof. J. Zhang, Prof. T. Chen  
 School of Chemical Sciences  
 University of Chinese Academy of Sciences  
 19A Yuquan Road, Beijing 100049, China

 The ORCID identification number(s) for the author(s) of this article can be found under <https://doi.org/10.1002/aisy.202000239>.

Prof. W. Lu  
 Guangdong Provincial Key Laboratory of Luminescence from Molecular Aggregates  
 South China University of Technology  
 Guangzhou 510640, China

Prof. S. Wu  
 Department of Polymer Science and Engineering  
 University of Science and Technology of China  
 No. 96 Jinzhai Road, Hefei 230026, China

© 2021 The Authors. Advanced Intelligent Systems published by Wiley-VCH GmbH. This is an open access article under the terms of the Creative Commons Attribution License, which permits use, distribution and reproduction in any medium, provided the original work is properly cited.

DOI: 10.1002/aisy.202000239

between the radiative rate of donor and the rate of energy transfer in fluorescence resonance energy transfer (FRET) microlasers.<sup>[4]</sup> Zhang et al. reported a set of phototunable trichromic fluorescent materials showing a dynamically tunable FRET process for secure data encryption.<sup>[3b]</sup> For a given 2D QR code printed by using the trichromic fluorescent materials as inks, dynamic images, which can be translated into different texts, were obtained by regulating UV irradiation time. Pan, Xia, and coworkers presented one kind of quantum dot-functionalized luminescent polydimethylsiloxane films (LPFs) with multistate tunable photoluminescence color that can be finely controlled by outer excitation power.<sup>[3c]</sup> Security level of information recorded in such LPFs-based 2D patterns could be improved significantly, because luminescent patterns of different colors (corresponding to different information) could be decrypted on demand by varying irradiation power. These impressive advances have demonstrated the huge potential of smart chromophoric/luminescent materials with multistate switching of coloration/fluorescence properties for high-level information protection and on-demand decryption.

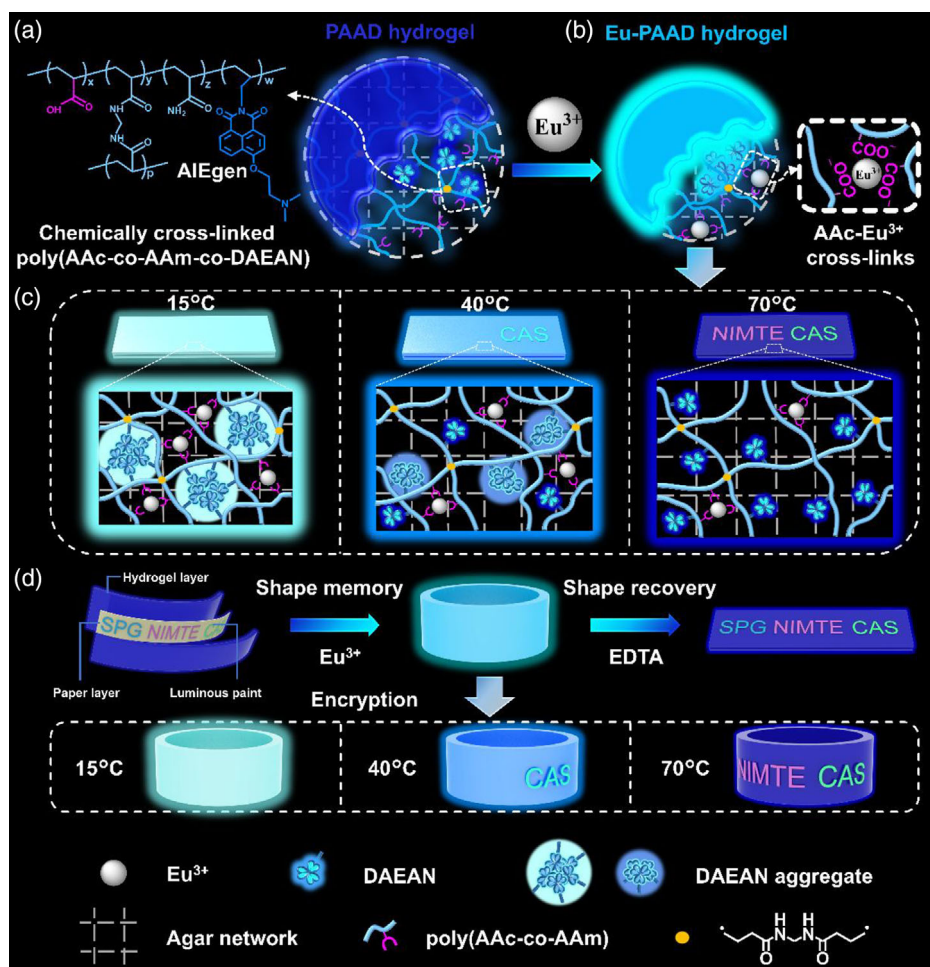
However, these reported chromophoric/luminescent materials-based anticounterfeiting systems, despite being state of the art, primarily encrypt information in single 2D planes and under utilize the possibility of encoding data into 3D structures to further enhance data security level and prevent counterfeiting. As have been evidenced in the recently reported 3D Janus plasmonic helical nanoaperture<sup>[5]</sup> and 3D surface-enhanced Raman-scattering anticounterfeiting systems,<sup>[1b,6]</sup> the elegant 3D information encryption platforms could provide many extra advantages than their traditional 2D counterparts, including more advanced encryption algorithms, enhanced decoding complexities, and probably larger encoding capacities. These superior advantages of 3D information encryption platforms would significantly increase the difficulty of getting access to the precoded information for counterfeiters, making them ideal candidates for high-level information encryption. Nevertheless, luminescent materials-based 3D information encryption platforms, despite being highly desired, still remain underdeveloped, probably because of the difficulty facing the design and preparation of robust materials with both well-tailored emission and versatile 2D/3D shape-programming capacities.

As a rising star of smart luminescent materials, stimuli-responsive fluorescent polymeric hydrogels (FPHs) have the potential to address these difficulties, because they can integrate the merits of both fluorescent materials and polymeric hydrogels. On the one hand, FPHs can be facilely tailored according to the chemical structure and composition, sensitivity to external stimuli, as well as dynamic fluorescence properties.<sup>[7]</sup> Therefore, fluorescent hydrogels have recently become one of the most prominent materials for smart confidential information protection.<sup>[8]</sup> For example, Wang's group utilized the ClO<sup>-</sup>/SCN<sup>-</sup>-triggered reversible response of luminescent Tb<sup>3+</sup>-nanocellulose hydrogels for latent fingerprint detection and encryption.<sup>[9]</sup> Sessler, Huang, and coworkers fabricated fluorescent hydrogels with supramolecular recognition motifs and demonstrated their use as building blocks to form various fluorescent code arrays via physical adhesion for information encoding, reading, and transforming.<sup>[10]</sup> Zhao, Li, and colleagues have recently reported another type of polymeric hydrogel block to construct

photocontrolled fluorescent code arrays for reversible information encryption and decryption.<sup>[11]</sup> These recent progresses demonstrate the huge potential of using luminescent hydrogels for secure information protection. On the other hand, FPHs can also be designed to have satisfying room-temperature shape memory and self-healing features by the introduction of reversible supramolecular interactions or dynamic covalent bonds.<sup>[12]</sup> These multifunctions, together with their soft and flexible natures,<sup>[13]</sup> enable FPHs to be facilely programmed into a myriad of complex 2D/3D structures.<sup>[14]</sup> Therefore, we envisage that new-concept 3D information encryption platforms with enhanced security level could be constructed by specially designed FPHs, thus revolutionizing the traditional fluorescence-based 2D anticounterfeiting platforms to more preferable 3D ones.

To verify our hypothesis, we have recently made an important attempt to construct perylene-tetracarboxylic acid-grafted gelatin/polyvinyl alcohol hydrogels with Fe<sup>3+</sup>-triggered fluorescence quenching, borax-triggered shape memory, and self-healing properties.<sup>[15]</sup> Using the origami technique, the first 3D fluorescent hydrogel origami for multistage data security protection was demonstrated, successfully extending data encryption capabilities from 2D to 3D. Nevertheless, the developed hydrogels, synthesized from the traditional perylene-tetracarboxylic acid (PTA) fluorophores, were only weakly fluorescent, due to aggregation-caused quenching (ACQ) nature of PTA molecules in quasisolid-state hydrogel systems. Moreover, hydrogels are primarily limited to the two-state switching of fluorescence property, that is, on-off emission response when triggered by Fe<sup>3+</sup> stimulus. These disadvantages would significantly restrict the possibility to enable on-demand decryption and transmission of information that are pre-encoded in 3D hydrogel structures.

Herein, we combine the aggregation-induced emission (AIE) mechanism<sup>[16]</sup> and dynamic metal-ligand coordination to prepare multifunctional programmable polymeric hydrogels with multistate fluorescence switching capabilities, followed by the fabrication of a more powerful 3D information encryption platform that allows for on-demand information decryption and transmission. As shown in **Scheme 1a**, the designed PAAD hydrogel has a typical double network structure, a physically cross-linked agar network, and a chemically cross-linked poly(AAc-co-AAm-co-DAEAN) network (featuring an upper critical solution temperature, UCST) prepared from radical copolymerization of 4-(dimethylamino)ethoxy-N-allyl-1,8-naphthalimide (DAEAN), acrylic acid (AAc), acrylamide (AAm), and methylene bisacrylamide crosslinker. DAEAN is a specially designed AIE monomer, in which the planar naphthalimide (NI) luminogens are substituted by the bulky dimethylaminoethoxy group to produce propeller-shaped molecular conformation that is in favor for AIE.<sup>[17]</sup> Due to the spontaneous aggregation of hydrophobic AIEgens in our hydrophilic hydrogel matrix, PAAD emits bright blue light. Their emission intensities can be further enhanced by subsequent complexation with Eu<sup>3+</sup> to produce Eu-PAAD hydrogels via AAc-Eu<sup>3+</sup> crosslinks by inducing a much heavier AIEgen aggregation (Scheme 1b). The dynamic and reversible AAc-Eu<sup>3+</sup> coordination can also be used as temporary crosslinks to program the hydrogel films into complex 3D temporary structures via shape memory process at room temperature. Moreover, benefiting from the unique lanthanide-coordinated polymer structure, the obtained Eu-PAAD hydrogels can be engineered to feature the desirable but rarely achieved



**Scheme 1.** Illustration showing the multistate fluorescence switching of AIE-active Eu-PAAD hydrogel and its use as 3D information encryption platforms for on-demand decryption. a) Illustration of PAAD hydrogel and its molecular structure. b) A scheme of Eu-PAAD hydrogel prepared by immersing PAAD hydrogel in  $\text{Eu}^{3+}$  solution to form AAc- $\text{Eu}^{3+}$  crosslinks. c) The proposed multistate fluorescence switching mechanism of Eu-PAAD hydrogel at different temperatures. As will be discussed later, the multistate fluorescence switching behavior of Eu-PAAD hydrogel is believed to come from the unsynchronized dissociation kinetics of hydrogen bonds and lanthanide coordination insertions over a wide temperature range. d) 3D information encryption platform for on-demand decryption. Specifically, one 2D information carrier was first developed by sandwiching two Eu-PAAD hydrogel films together with one paper with prewritten information using commercially available luminous paints of blue, green, and red emission color, respectively. Such 2D information carriers were then folded into 3D cylinder shapes by hands and then immersed into  $\text{Eu}^{3+}$  solutions to produce a 3D anticounterfeiting platform via shape memory and self-healing processes. Different information would be disclosed at different temperatures. But the whole information cannot be encoded unless EDTA was used to induce shape recovery from 3D to 2D.

multistate fluorescence switching behavior through thermo-triggered stepwise dissociation of lanthanide coordination interaction and hydrogen bonds (Scheme 1c). These properties together have allowed us to program the multistate AIE-active Eu-PAAD hydrogel into a high-level 3D anticounterfeiting platform with on-demand information decryption capacities. As shown in Scheme 1d, the information that was preprinted onto papers using luminous paints of various colors could be encrypted into a 3D cylinder-shaped hydrogel structure via a combination of shape memory and self-healing properties. Due to the multistate fluorescence switching ability of Eu-PAAD hydrogels, on-demand decryption of the encoded information was then realized by the control of environment temperature, which can be further used to send manifold customized messages to multiple receivers.

## 2. Results and Discussion

### 2.1. Fabrication of the AIE-Active Eu-PAAD Hydrogels

The key step to preparing the hydrogel is the design and synthesis of the aggregation-induced emissive DAEAN monomer. Its synthetic route is shown in Figure S1, Supporting Information. 4-Bromo-N-allyl-1,8-naphthalimide was first obtained according to the reported method<sup>[17]</sup> and subsequently allowed to react with excess *N,N*-dimethylethanolamine to produce DAEAN as a yellowish powder. Its chemical structure was verified by proton nuclear magnetic resonance spectroscopy ( $^1\text{H}$  NMR) (Figure S2a, Supporting Information), carbon nuclear magnetic resonance spectroscopy ( $^{13}\text{C}$  NMR) (Figure S2b, Supporting



Information), and Fourier transform infrared (FTIR) spectra (Figure S3, Supporting Information). DAEAN is readily soluble in DMSO, DMF, THF, CHCl<sub>3</sub>, and methanol but is only partially soluble in H<sub>2</sub>O (about 0.1 mg mL<sup>-1</sup>) at room temperature. Its photoluminescence spectra were subsequently investigated in methanol/water by changing the water fraction of the solvent mixture to tune the extent of solute aggregation. As shown in Figure S4 and S5, Supporting Information, DAEAN is weakly fluorescent in pure methanol solution but displays remarkable emission enhancement with an increase of the water fraction in the solvent mixture, clearly revealing the AIE feature of DAEAN monomer. Further evidence of its AIE nature comes from the concentration-dependent fluorescence spectra, which reveal that the emission intensity of aqueous DAEAN solutions is in direct proportion to the monomer concentration (0.001–0.02 mg mL<sup>-1</sup>) (Figure S6 and S7, Supporting Information).

AIE hydrogel was then prepared from this specially designed DAEAN monomer. Typically, DAEAN was codissolved with AAC, AAm, methylene-bis-acrylamide crosslinker, and agar in hot water. Thermally induced free radical polymerization of the mixture was subsequently conducted in a self-made mold to produce PAAD hydrogels, which were soaked into Eu<sup>3+</sup> ions solution (0.1 M) to induce the formation of AAC-Eu<sup>3+</sup> crosslinks. Aggregation-induced emissive Eu-PAAD hydrogels were then obtained by transferring the as-prepared hydrogels into a large amount of pure water to remove excess Eu<sup>3+</sup>. As shown in

Figure 1a, Eu-PAAD has a typical double network structure: a cross-linked agar network via hydrogen bonds and poly(AAc-co-AAm-co-DAEAN) network via both chemical and metal-coordination crosslinks. To make the possible modulation of the fluorescent features via changes in the AIEgen content, a family of hydrogel samples (I–III) was synthesized by varying the feed ratio (Table S1, Supporting Information). All of the hydrogel samples emit bright blue fluorescence when illuminated under UV light at 365 nm (Figure S8, Supporting Information). Their emission intensities increase with increasing content of DAEAN and are significantly higher than that of the corresponding PAAD hydrogels (Figure 1b), because the additional AAC-Eu<sup>3+</sup> crosslinks result in heavier aggregation of substituted naphthalimide AIEgens. A similar emission enhancement has also been observed upon Tb<sup>3+</sup> complexation but not for Ca<sup>2+</sup> (Figure S9, Supporting Information), because of the relatively weaker complexation capacity of Ca<sup>2+</sup> than Tb<sup>3+</sup> and Eu<sup>3+</sup>. This speculation was further evidenced by transmittance, FTIR, scanning electron microscope (SEM), rheological, and tensile measurements. To facilitate the studies, sample III with the highest fluorescence intensity (Figure S8, Supporting Information) and solid content of 57.50 ± 0.30% were taken as an example. Unless otherwise specified, PAAD (its DAEAN content was calculated to be 0.008 mg mL<sup>-1</sup> from the UV-vis measurements shown in Figure S10, Supporting Information) and Eu-PAAD hydrogel samples reported in this manuscript are prepared from this feed

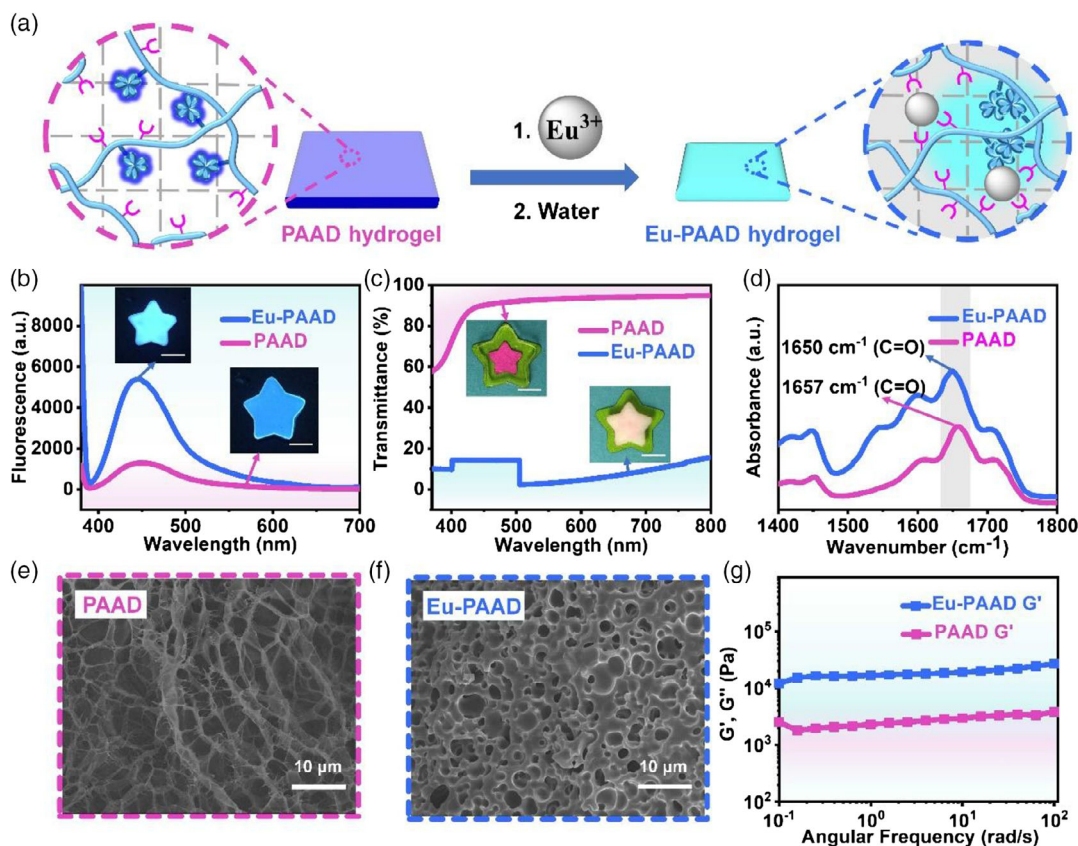


**Figure 1.** a) Preparation of Eu-PAAD hydrogel via Eu<sup>3+</sup> complexation. b) Fluorescence and c) transmittance spectra of PAAD and Eu-PAAD hydrogels. Inset photos were taken under 365 nm UV light and in day light, respectively. d–f) FTIR spectra and SEM images of the freeze-dried PAAD and Eu-PAAD hydrogel samples. g) Rheological measurement of PAAD and Eu-PAAD hydrogels. Scale bars in digital photos are 1 cm.

formula. As shown in Figure 1c, upon  $\text{Eu}^{3+}$  coordination, the hydrogel soon becomes opaque, which is evidenced by the large transmittance loss. The stretching vibration frequency of carbonyl groups shifts from 1657 to 1650  $\text{cm}^{-1}$  in the IR spectra of freeze-dried PAAD and Eu-PAAD hydrogel samples (Figure 1d), indicating the formation of metal coordination interactions between  $\text{Eu}^{3+}$  and carboxyl groups grafted on the hydrogels.<sup>[18]</sup> Meanwhile, the SEM image of the freeze-dried PAAD sample (Figure 1e) shows a loosely porous cross-linked network, in contrast to much smaller porous structures observed for Eu-PAAD (Figure 1f), due to the formation of high-density AAc- $\text{Eu}^{3+}$  crosslinks. These results are consistent with rheological (Figure 1g) and tensile (Figure S11, Supporting Information) measurements, which indicate a much larger storage modulus ( $G'$ ) and stretchability after  $\text{Eu}^{3+}$  coordination.

Due to the dynamic AAc- $\text{Eu}^{3+}$  coordination interactions, PAAD hydrogels are also endowed with shape memory and self-healing properties. To this end, the classic shape memory experiments were conducted, in which the PAAD hydrogel stripe was bent by external forces and placed into  $\text{Eu}^{3+}$  solutions to form temporary AAc- $\text{Eu}^{3+}$  crosslinks at room temperature. It is found that the shape memory ratios increase over time and reaches about 80% within 1 h (Figure 2a). When PAAD hydrogels were originally molded into various 2D shapes, they could be then programmed to perform more complex 2D-to-3D shape memory behaviors and be fixed as such temporary profiles as cuttlefish (Figure 2b), butterfly, or triple helix (Figure S12 and S13, Supporting Information). To demonstrate its self-healing

property, the more complex butterfly-on-flower-type 3D hydrogel structure was constructed by two-step procedures, in which 3D hydrogel flower and butterfly structures were first prepared in the shape memory process and then self-healed together via AAc- $\text{Eu}^{3+}$  coordination interactions (Figure 2c).

## 2.2. Multistate Fluorescence Switching Capacities of Eu-PAAD Hydrogels

Interestingly, the developed Eu-PAAD hydrogels are proved to be UCST-type by transmittance experiments (Figure 3a), which suggests a gradually increasing transmittance over a wide temperature range (25–60 °C). This behavior is in contrast to that of the previously reported poly(AAc-co-AAm) hydrogels that have a relatively narrow volume phase transition between 30 and 40 °C.<sup>[19]</sup> This broad and continuous transmittance response over a wide temperature range is believed to result from the unsynchronized dissociation kinetics of hydrogen bonds and lanthanide coordination interactions of the specially designed  $\text{Eu}^{3+}$ -coordinated poly(AAc-co-AAm) network in our hydrogels. Specifically, upon temperature increase, the vast hydrogen bonds between PAAc and PAAm segments in the Eu-PAAD hydrogels quickly dissociate to enhance the solvation of polymer chains, whereas AAc- $\text{Eu}^{3+}$  coordination interactions require a relative higher temperature for gradual dissociation, leading to the continuously adjustable transmittance properties of Eu-PAAD hydrogels over a wide temperature range. This continuous and reversible (Figure S14, Supporting Information) temperature-dependent transmittance

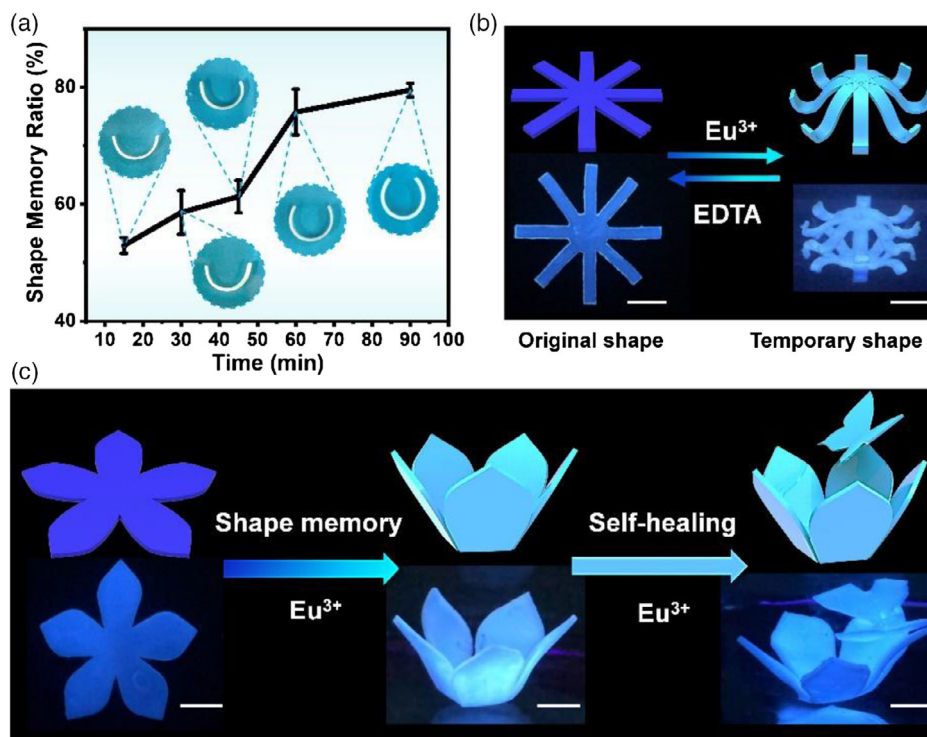


**Figure 2.** a) Shape fixity ratios of the PAAD hydrogel at different shape memory times in aqueous  $\text{Eu}^{3+}$  solution (0.1 M) at 25 °C. b) Fabrication of a 3D cuttlefish-shaped hydrogel structure by starting with one tailored 2D hydrogel piece via shape memory. c) Fabrication of the complex 3D hydrogel structure (butterfly perching on the flower) by starting with two tailored 2D hydrogel pieces via the combination of shape memory and self-healing abilities at room temperature (photos taken under 365 nm illumination). Scale bars in digital photos are 1 cm.

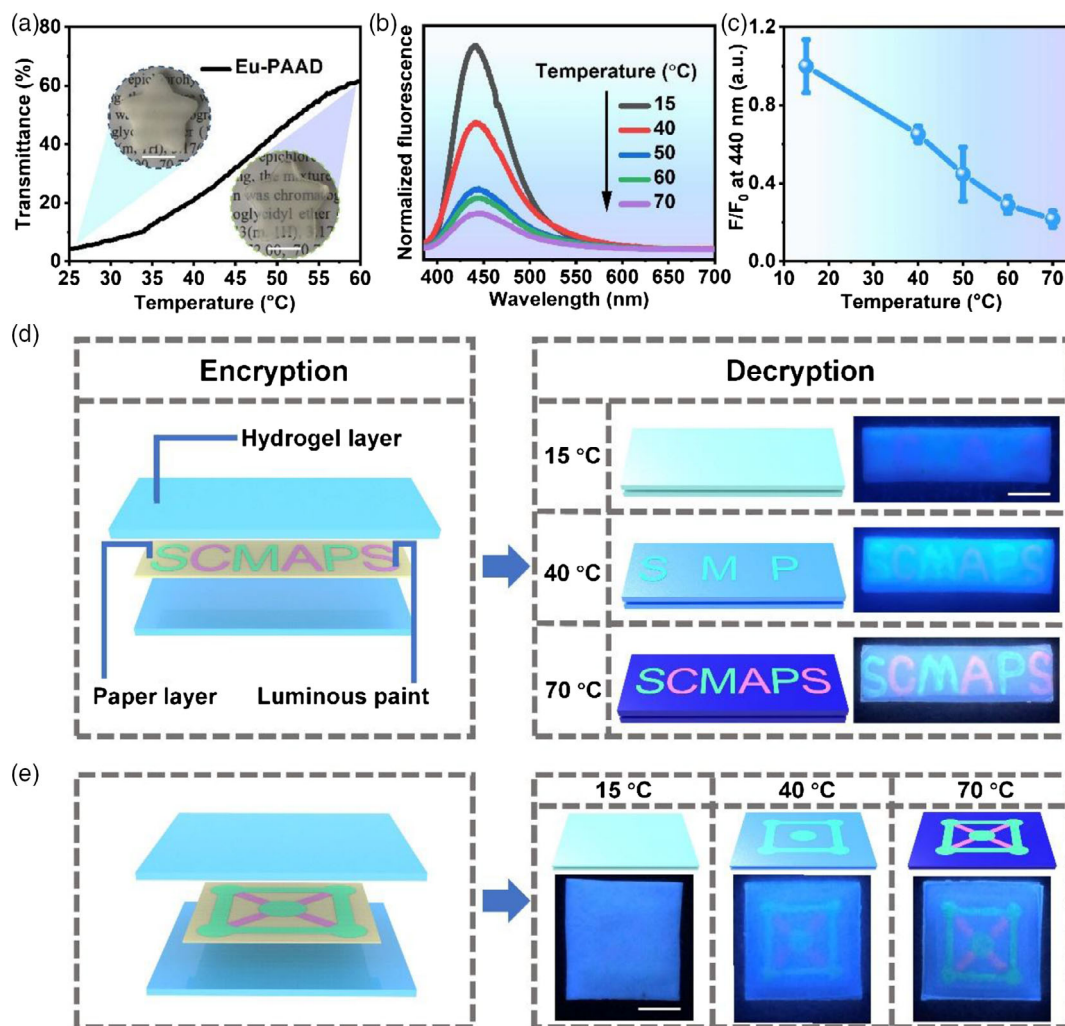


**Figure 3.** Multistate switching of Eu-PAAD hydrogel. a) Temperature-dependent transmittance curve (photos taken under day light at 25 and 60 °C). b) Normalized fluorescence spectra recorded at different temperatures (excitation at 365 nm). c) Peak emission intensity ratio ( $F/F_0$ ) of Eu-PAAD hydrogel at 440 nm as a function of temperature. d,e) 2D anticounterfeiting platform for on-demand decryption, which was first developed by sandwiching two Eu-PAAD hydrogel films together with one paper containing information. Different information would appear at different temperatures. Photos in (d,e) were taken on the heating table under a 365 nm UV lamp. Scale bars are 1 cm.

responses of Eu-PAAD hydrogels make it possible to realize the important but rarely realized multistate switching of fluorescence properties. As shown in Figure 3b,c and S15, upon temperature increase, the intensity of the second state (40 °C) drops by 30% compared with that of the initial state (15 °C). In the latter state (50 °C), intensity decreases by nearly 50%. When elevating temperature to 70 °C, the intensity drops by over 80%. This multistate fluorescence feature should be ascribed to the gradually increasing solvation of polymer chains that leads to the gradually decreasing aggregation of AIEgens, as evidenced by the less storage modulus at a higher temperature (Figure S16, Supporting Information).

Such unique multistate fluorescence switching capacities of our Eu-PAAD hydrogels thus encouraged us to explore their potential in high-level information encryption and on-demand decryption. As a proof of concept, a 2D anticounterfeiting device was first developed by sandwiching two Eu-PAAD hydrogel films together with one paper (Figure 3d), on which “SMP” and “CAS” information were prewritten using commercially available

luminous paints of green and red emission color, respectively. In the designed 2D anticounterfeiting device, the two Eu-PAAD hydrogel films were stuck together via self-healing interaction. It should be noted that green light-emissive paint is brighter than red light-emissive paint. At a lower temperature (15 °C), Eu-PAAD hydrogel films are highly emissive, which significantly block the transmission of the information encoded onto the middle paper layer (Figure S17, Supporting Information). As a result, such information encrypted in this 2D anticounterfeiting device cannot be directly read under simple UV light illumination, indicating its superior data security to their traditional counterparts with static fluorescence output only. Next, when elevating temperature to 40 °C, the emission intensity of the hydrogel layer significantly decreases. At this condition, the first-level “SMP” message written by brighter green light-emissive paint becomes visible under UV light illumination. Then, upon continuous temperature increase to 70 °C, emission intensity of the hydrogel layer is largely weakened, thus



allowing the whole information to be accessed under UV light. Similar anticounterfeiting devices were further constructed for other information (Figure 3e and S18 and S19, Supporting Information). In these demonstrations, different messages could be stepwise decrypted due to the unique thermo-triggered multistate fluorescence switching features of our Eu-PAAD hydrogels. Notably, this on-demand information decryption can only be conducted by an authorized individual who has knowledge of not only the correct encryption key, but also exact temperature.

### 2.3. Fluorescence-Based 3D Anticounterfeiting Platform for On-Demand Information Decryption and Transmission

To further enhance encoding security level, more promising 3D information encryption platforms with on-demand decryption

features were then developed by a combination of shape memory and multistate fluorescence switching properties. As shown in Figure 4a, one butterfly-shaped 2D anticounterfeiting device was first folded into the 3D shape by hands and placed into  $\text{Eu}^{3+}$  solutions for a while to fix the temporary 3D shape via  $\text{AAC-Eu}^{3+}$  coordination interactions. In this way, the predesigned data were successfully decrypted into one 3D butterfly-shaped hydrogel structure. At a lower temperature, this encoded information written by luminous paint of various colors could not be accessed under UV light illumination because they were completely blocked by the intense AIE of Eu-PAAD hydrogel layer. When elevating the temperature to  $40^\circ\text{C}$ , partial information is revealed, whereas more information appears at  $70^\circ\text{C}$ . Nevertheless, whole information cannot be accessed unless the EDTA-triggered shape recovery process is conducted. As additional shape memory properties were utilized to fabricate the 3D encryption platform, the data security level is thus further

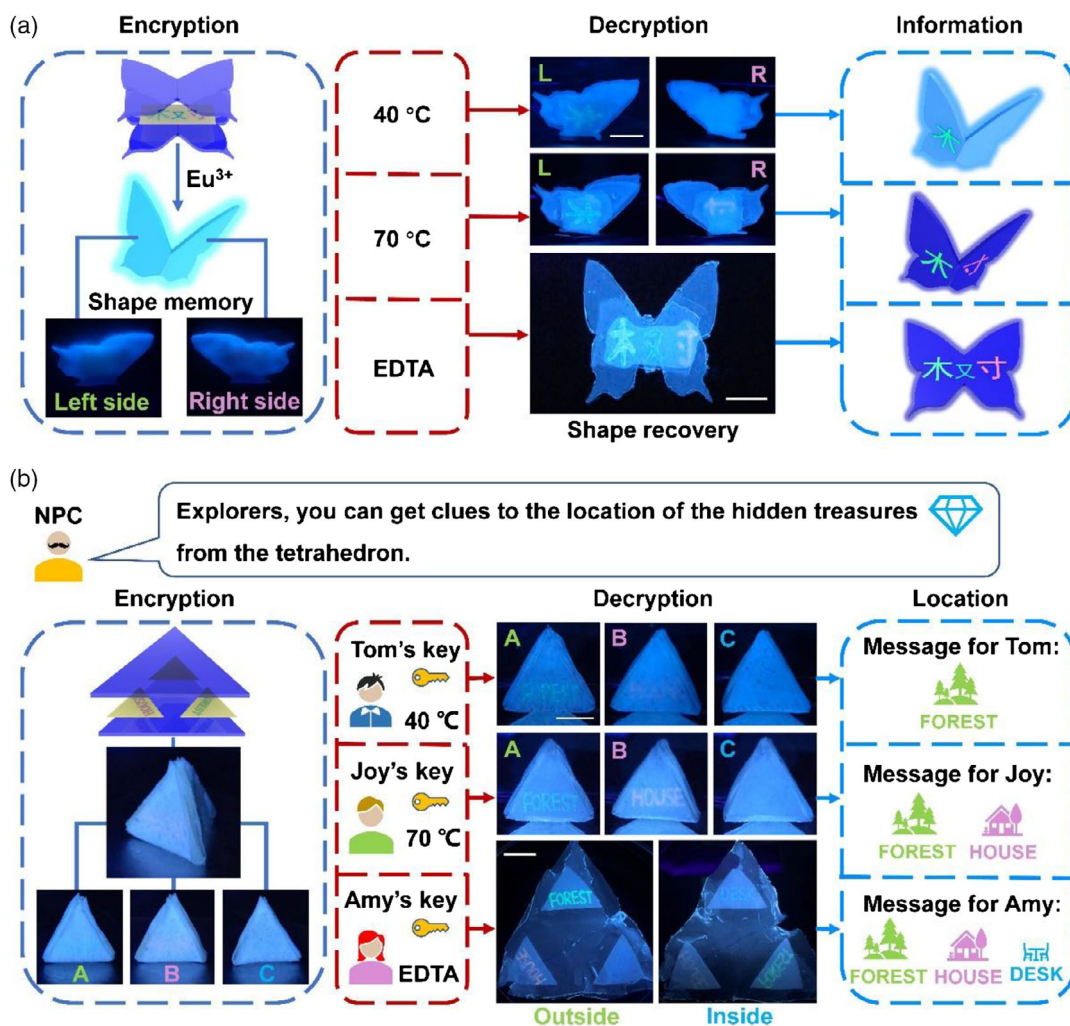


**Figure 4.** a) 3D anticounterfeiting platform for on-demand decryption, which was prepared by folding 2D information carrier into 3D shape by hands and then immersed into  $\text{Eu}^{3+}$  solutions to fix such 3D structures. Different information would appear at  $15^\circ\text{C}$  (nothing),  $40^\circ\text{C}$  (“木”), and  $70^\circ\text{C}$  (“村”). But the whole information (“树”) cannot be encoded unless EDTA is used to induce shape recovery from 3D to 2D. b) 3D encryption platform for on-demand information transmission. In a treasure hunt game, the NPC would like to send different messages to multiple receivers. To do this, three identical 3D hydrogel encryption devices were first prepared and then sent to Tom, Joy, and Amy. Customer-specific messages would be disclosed using customized keys (photos taken under 365 nm illumination). Scale bars are 1 cm.

enhanced compared with its 2D counterparts. On the basis of similar design principles, the 3D decryption platform could be generally used for the safe protection and on-demand decryption of other information (Figure S20, Supporting Information).

On the basis of the developed high-level 3D anticounterfeiting platforms, in which different information can be decrypted under different conditions, we further explore the possibility to develop a highly secure scheme for on-demand data transmission. As shown in Figure 4b, in a treasure hunt game, the nonplayer character (NPC) would like to send different messages to multiple receivers (e.g., Tom, Joy, Amy). To this end, he first prepared 2D triangle-shaped information carriers by sandwiching two PAAD hydrogel films together with one paper containing these messages. Such 2D information carriers were then folded into a 3D tetrahedron shape by hands and then immersed into  $\text{Eu}^{3+}$  ions for simultaneous self-repair and shape memory. In this way, the initial 2D information carriers were successfully programmed to free-standing 3D tetrahedron-shaped hydrogel structures, which are stabilized by dynamic AAC- $\text{Eu}^{3+}$  interactions. The as-prepared 3D hydrogel structures are highly luminescent at room temperature, making the predesigned messages successfully encrypt inside the 3D hydrogel geometries. Three identical 3D hydrogel encryption devices were then sent to Tom, Joy, and Amy. After receipt of NPC samples, together with the customized keys, Tom finds “Forest” by elevating the temperature to 40 °C. Joy reads out “House, Forest” at 70 °C. Amy obtains “Desk, House, Forest” after unfolding the 3D hydrogel structures in EDTA solutions, which break AAC- $\text{Eu}^{3+}$  coordination crosslinks to induce simultaneous shape and fluorescence recovery. Following a similar design, other messages encoded in 3D hydrogel structures of various shapes can be deciphered and transmitted to different receivers using the provided keys (Figure S21, Supporting Information). In other words, a myriad of messages could be decoded by one single 3D hydrogel encryption design, given that the sequences of keys are customized. This suggests an unprecedented security for on-demand information transmission, especially to multiple receivers.

### 3. Conclusion

In conclusion, we have presented a new-type multifunctional Eu-PAAD hydrogel with multistate fluorescence switching capacities via the AIE mechanism and dynamic lanthanide coordination interaction. The materials are prepared by copolymerizing a specially designed AIE-active DAEM monomer into a chemically cross-linked poly(AAc-co-AAm) network (featuring a typical UCST) that are interpenetrated with the physically cross-linked agar network, followed by  $\text{Eu}^{3+}$  complexation to form lanthanide coordinated polymer segments via AAC- $\text{Eu}^{3+}$  crosslinks. These unique kinds of chemical structures endow Eu-PAAD hydrogel with satisfying shape memory, self-healing, and especially thermo-responsive multistate fluorescence switching properties. Based on the synergetic effect of these promising properties, the high-level 3D data encoding platform has been demonstrated, in which information prewritten by luminous paints of various colors can be safely encrypted into 3D hydrogel structures of various shapes. Particularly, such information could be subject to stepwise decryption at different conditions (e.g., different temperatures or EDTA treatment), which can be further used

for on-demand information transmission to multiple receivers. Notably, such on-demand information decryption and transmission process can only be conducted by an authorized individual who has knowledge of not only the correct encryption key, but also exact temperature, indicating the much-higher encryption safety of our 3D platform than its classic 2D counterparts. Our findings further highlight the tremendous potential of fluorescence-based 3D anticounterfeiting structures for high-level information encryption and on-demand decryption.

### Supporting Information

Supporting Information is available from the Wiley Online Library or from the author.

### Acknowledgements

The authors thank National Natural Science Foundation of China (52073297, 21774138, 51773215), Key Research Program of Frontier Sciences, Chinese Academy of Sciences (QYZDB-SSW-SLH036), the National Key Research and Development Program of China (2018YFB1105100), Youth Innovation Promotion Association of Chinese Academy of Sciences (2019297), the Open Fund of Guangdong Provincial Key Laboratory of Luminescence from Molecular Aggregates, and South China University of Technology (2019B030301003).

### Conflict of Interest

The authors declare no conflict of interest.

### Keywords

aggregation-induced emissions, information encryptions, multistate fluorescence switching, on-demand decryptions, three-dimensional hydrogel structures

Received: October 16, 2020

Revised: November 23, 2020

Published online: February 5, 2021

- [1] a) R. Arppe, T. J. Sørensen, *Nat. Rev. Chem.* **2017**, *1*, 1; b) G. C. Phan-Quang, X. Han, C. S. L. Koh, H. Y. F. Sim, C. L. Lay, S. X. Leong, Y. H. Lee, N. Pazos-Perez, R. A. Alvarez-Puebla, X. Y. Ling, *Acc. Chem. Res.* **2019**, *52*, 1844; c) L. Gu, H. Shi, L. Bian, M. Gu, K. Ling, X. Wang, H. Ma, S. Cai, W. Ning, L. Fu, H. Wang, S. Wang, Y. Gao, W. Yao, F. Huo, Y. Tao, Z. An, X. Liu, W. Huang, *Nat. Photonics* **2019**, *13*, 406.
- [2] a) O. Guillou, C. Daigebonne, G. Calvez, K. Bernot, *Acc. Chem. Res.* **2016**, *49*, 844; b) X. Qin, J. Xu, Y. Wu, X. Liu, *ACS Cent. Sci.* **2019**, *5*, 29; c) J. Andreasson, U. Pischel, *Chem. Soc. Rev.* **2018**, *47*, 2266; d) S. Wei, Z. Li, W. Lu, H. Liu, J. Zhang, T. Chen, B. Z. Tang, *Angew. Chem. Int. Ed.* **2020**, *59*, <https://doi.org/10.1002/anie.202007506>.
- [3] a) Y. Ma, Y. Yu, P. She, J. Lu, S. Liu, W. Huang, Q. Zhao, *Sci. Adv.* **2020**, *6*, eaaz2386; b) W. Tian, J. Zhang, J. Yu, J. Wu, J. Zhang, J. He, F. Wang, *Adv. Funct. Mater.* **2018**, *28*, 1703548; c) F. Li, X. Wang, Z. Xia, C. Pan, Q. Liu, *Adv. Funct. Mater.* **2017**, *27*, 1700051; d) C. Shi, X. Shen, Y. Zhu, X. Li, Z. Pang, M. Ge, *ACS Appl. Mater. Interfaces* **2019**, *11*, 18548; e) J. Wang, J. Ma, J. Zhang, Y. Fan, W. Wang, J. Sang, Z. Ma, H. Li, *ACS Appl. Mater. Interfaces* **2019**,



- 11, 35871; f) Y. Ma, Y. Dong, S. Liu, P. She, J. Lu, S. Liu, W. Huang, Q. Zhao, *Adv. Opt. Mater.* **2020**, *8*, 1901687.
- [4] Z. Gao, K. Wang, Y. Yan, J. Yao, Y. S. Zhao, *Natl. Sci. Rev.* **2020**, nwaal62.
- [5] Y. Hu, X. Luo, Y. Chen, Q. Liu, X. Li, Y. Wang, N. Liu, H. Duan, *Light: Sci. Appl.* **2019**, *8*, 86.
- [6] Y. Liu, Y. H. Lee, M. R. Lee, Y. Yang, X. Y. Ling, *ACS Photonics* **2017**, *4*, 2529.
- [7] a) L. Hu, Q. Zhang, X. Li, M. J. Serpe, *Mater. Horiz.* **2019**, *6*, 1774; b) C. Lowenberg, M. Balk, C. Wischke, M. Behl, A. Lendlein, *Acc. Chem. Res.* **2017**, *50*, 723; c) H. Yuk, B. Lu, X. Zhao, *Chem. Soc. Rev.* **2019**, *48*, 1642; d) T. Matsuda, R. Kawakami, R. Namba, T. Nakajima, J. P. Gong, *Science* **2019**, *363*, 504.
- [8] a) X. Ji, Z. Li, X. Liu, H. Q. Peng, F. Song, J. Qi, J. W. Y. Lam, L. Long, J. L. Sessler, B. Z. Tang, *Adv. Mater.* **2019**, *31*, e1902365; b) C. N. Zhu, T. Bai, H. Wang, W. Bai, J. Ling, J. Z. Sun, F. Huang, Z. L. Wu, Q. Zheng, *ACS Appl. Mater. Interfaces* **2018**, *10*, 39343; c) Q. Zhu, K. Vliet, N. Holten Andersen, A. Miserez, *Adv. Funct. Mater.* **2019**, *29*, 1808191; d) J. Hai, H. Wang, P. Sun, T. Li, S. Lu, Y. Zhao, B. Wang, *ACS Appl. Mater. Interfaces* **2019**, *11*, 44664; e) H. S. Kang, S. W. Han, C. Park, S. W. Lee, H. Eoh, J. Baek, D.-G. Shin, T. H. Park, J. Huh, H. Lee, D. E. Kim, D. Y. Ryu, E. L. Thomas, W.-G. Koh, C. Park, *Sci. Adv.* **2020**, *6*, eabb5769.
- [9] J. Hai, T. Li, J. Su, W. Liu, Y. Ju, B. Wang, Y. Hou, *Angew. Chem. Int. Ed.* **2018**, *57*, 6786.
- [10] X. Ji, R. T. Wu, L. Long, X. S. Ke, C. Guo, Y. J. Ghang, V. M. Lynch, F. Huang, J. L. Sessler, *Adv. Mater.* **2018**, *30*, 1705480.
- [11] Z. Li, H. Chen, B. Li, Y. Xie, X. Gong, X. Liu, H. Li, Y. Zhao, *Adv. Sci.* **2019**, *6*, 1901529.
- [12] W. Lu, X. Le, J. Zhang, Y. Huang, T. Chen, *Chem. Soc. Rev.* **2017**, *46*, 1284.
- [13] Y. Wu, H. Wang, F. Gao, Z. Xu, F. Dai, W. Liu, *Adv. Funct. Mater.* **2018**, *28*, 1801000.
- [14] a) Y. Zhang, J. Liao, T. Wang, W. Sun, Z. Tong, *Adv. Funct. Mater.* **2018**, *28*, 1707245; b) Z. Zhao, S. Zhuo, R. Fang, L. Zhang, X. Zhou, Y. Xu, J. Zhang, Z. Dong, L. Jiang, M. Liu, *Adv. Mater.* **2018**, *30*, e1804435; c) M. Liu, Y. Ishida, Y. Ebina, T. Sasaki, T. Hikima, M. Takata, T. Aida, *Nature* **2015**, *517*, 68; d) X. Peng, T. Liu, Q. Zhang, C. Shang, Q. W. Bai, H. Wang, *Adv. Funct. Mater.* **2017**, *27*, 1701962; e) K. Sano, Y. Ishida, T. Aida, *Angew. Chem. Int. Ed.* **2018**, *57*, 2532; f) X. Ji, B. Shi, H. Wang, D. Xia, K. Jie, Z. L. Wu, F. Huang, *Adv. Mater.* **2015**, *27*, 8062; g) Y. Zhang, H. Gao, H. Wang, Z. Xu, X. Chen, B. Liu, Y. Shi, Y. Lu, L. Wen, Y. Li, Z. Li, Y. Men, X. Feng, W. Liu, *Adv. Funct. Mater.* **2018**, *28*, 1705962; h) Y. Wang, W. Huang, Y. Wang, X. Mu, S. Ling, H. Yu, W. Chen, C. Guo, M. C. Watson, Y. Yu, L. D. Black, 3rd, M. Li, F. G. Omenetto, C. Li, D. L. Kaplan, *Proc. Natl. Acad. Sci. USA* **2020**, *117*, 14602; i) J. H. Kang, H. Kim, C. D. Santangelo, R. C. Hayward, *Adv. Mater.* **2019**, *31*, e0193006; j) S. Wei, W. Lu, X. Le, C. Ma, H. Lin, B. Wu, J. Zhang, P. Theato, T. Chen, *Angew. Chem. Int. Ed.* **2019**, *58*, 16243; k) W. Fan, C. Shan, H. Guo, J. Sang, R. Wang, R. Zheng, K. Sui, Z. Nie, *Sci. Adv.* **2019**, *5*, 1; l) A. K. Mishra, T. J. Wallin, W. Pan, P. Xu, K. Wang, E. P. Giannelis, B. Mazzolai, R. F. Shepherd, *Sci Robot.* **2020**, *5*, 1; m) X. Du, H. Cui, Q. Zhao, J. Wang, H. Chen, Y. Wang, *Research* **2019**, 2019, 1; n) H. Qin, T. Zhang, N. Li, H. P. Cong, S. H. Yu, *Nat. Commun.* **2019**, *10*, 2202; o) F. G. Downs, D. J. Lunn, M. J. Booth, J. B. Sauer, W. J. Ramsay, R. G. Klempner, C. J. Hawker, H. Bayley, *Nat. Chem.* **2020**, *12*, 363.
- [15] Y. Zhang, X. Le, Y. Jian, W. Lu, J. Zhang, T. Chen, *Adv. Funct. Mater.* **2019**, *29*, 1905514.
- [16] J. Mei, N. L. Leung, R. T. Kwok, J. W. Lam, B. Z. Tang, *Chem. Rev.* **2015**, *115*, 11718.
- [17] H. Liu, S. Wei, H. Qiu, B. Zhan, Q. Liu, W. Lu, J. Zhang, T. Ngai, T. Chen, *Macromol. Rapid Commun.* **2020**, *41*, e2000123.
- [18] W. Lu, C. Ma, D. Zhang, X. Le, J. Zhang, Y. Huang, C.-F. Huang, T. Chen, *J. Phys. Chem. C* **2018**, *122*, 9499.
- [19] J. Zheng, P. Xiao, X. Le, W. Lu, P. Théato, C. Ma, B. Du, J. Zhang, Y. Huang, T. Chen, *J. Mater. Chem. C* **2018**, *6*, 1320.